Molecular Dynamics Study of the Methanol Effect on the Membrane Morphology of Perfluorosulfonic Ionomers

Shingo Urata,* Jun Irisawa, and Akira Takada

Research Center, Asahi Glass Co., Ltd. (AGC), 1150 Hazawa-cho, Kanagawa-ku, Yokohama, Kanagawa 221-8755, Japan

Wataru Shinoda, Seiji Tsuzuki, and Masuhiro Mikami

National Institute of Advanced Industrial Science and Technology (AIST), 1-1-1 Umezono, Tsukuba, Ibaraki 305-8568, Japan

Received: May 20, 2005; In Final Form: July 8, 2005

The membranes of a perfluorosulfonic acid polymer swollen in 10−80 wt % methanol solution were investigated to elucidate the methanol effect on their morphologies, such as size of the solvent cluster, solvent location, and polymer structure, by using isothermal−isobaric molecular dynamics simulations. In higher methanol concentrations, we found less-spherical solvent aggregation and a more spread polymer structure because of the ampholytic nature of methanol. The partial radial distribution functions between solvent oxygen and fluorocarbons, which are composed of the main chain, clearly show that methanol is located closer to the polymer matrix than water. On the other hand, water is preferentially located in the vicinity of an acidic headgroup, SO_3^-, compared with methanol, although both have similar attractive interaction energies to the acidic group. Furthermore, we discussed solvent dynamics and hydrogen bonding between sulfonic oxygen and solvent O−H groups.

1. Introduction

There has been great interest in perfluorosulfonic acid polymers, such as Flemion and Nafion, as exchange membranes in polymer electrolyte membrane fuel cells (PEMFCs).[1] For the practical application of PEMFCs, membrane hydration is critical to the proton conductivity because it enhances proton dissociation and is attributed to form continuous clusters for proton transfer. The studies of small-angle X-ray and neutron scatterings (SAXS, SANS)[2−11] and several imaging observations[12,13] have suggested that the cluster is composed of several nanometer-sized water clusters joined together through narrow channels. On the other hand, in the direct methanol fuel cell (DMFC) system, the water path causes methanol transport through the membrane to the cathode, known as methanol crossover.[14−17] This phenomenon is one of the serious problems for the practical application of the membranes to the DMFC technology because it is responsible for fuel loss and cell potential reduction due to mixed potential at the cathode. The problem is accelerated by higher methanol concentration of solution.

An understanding of the morphology of the membranes swelling in methanol or a water/methanol mixture is thus a key factor for DMFC development. However, experimental investigations of the membranes swelling in methanol solution are very limited,[18−21] and the features of the swollen membrane in water/methanol mixtures have not yet been sufficiently revealed in comparison with those of the water-uptake membrane. In addition, there are few theoretical investigations of the membranes solvated in methanol and water/methanol mixtures,[22−24] although the water-swollen membranes of the ionomers have already been examined by a number of computational methods.[25−37] The previous theoretical studies have investigated an oligomer conformation of the perfluorosulfonic acid polymer in methanol[22] or methanol solution[23] and the intermolecular interactions between the pendant side chain and methanol;[24] however, the swollen membrane in methanol solution has not been studied.

In this study, we therefore investigate the membranes swelling in water/methanol mixtures by means of molecular dynamics (MD) simulations. This is a subsequent study to our previous paper that analyzed the membrane morphologies of 5−40 wt % water-uptake membranes.[32] As we especially focused our attention on methanol concentration dependence of the membrane morphology, we carried out a series of MD simulations for the membranes swelling in solution at six different methanol concentrations in the range 10−80 wt %.

We will discuss the methanol effect on the membrane morphology in the first subsection of the Results and Discussion. In that subsection, the methanol effect on (1) size of the solvent cluster, (2) solvent location, and (3) polymer structure is reported in detail. Subsequently, the methanol effect on hydrogen bonding between solvent hydrogen and sulfonic oxygen is investigated. Solvent dynamics is also analyzed as a function of methanol concentration.

2. Computational Methods

The membranes of perfluorinated ionomers immersed in 10, 20, 30, 40, 60, and 80 wt % methanol solution were modeled, and their MD simulations were carried out in the isothermal−isobaric ensemble. The total number of solvent molecules was set to be the same as in the case of the 20 wt % water-uptake membrane investigated in our previous study.[32] The simulated conditions are summarized in Table 1.

Because the details of model and force field parameters have already been explained in our previous study,[32] we briefly describe them here. Intermolecular interactions were modeled with Lennard-Jones (LJ) potentials and Coulombic interactions. The Ewald method[38] was used for the calculation of Coulomb interactions. The LJ interactions and real-space Ewald terms

* Corresponding author. Tel: +81-045-374-7074. Fax: +81-045-374-8730. E-mail: shingo-urata@agc.co.jp.

10.1021/jp052647h CCC: $30.25
Published on Web 08/18/2005

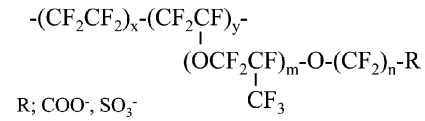

Figure 1. Schematic illustration of perfluorinated ionomers.

TABLE 1: Summary of Simulated Conditions

	methanol concn (wt %)						
	0[a]	10	20	30	40	60	80
no. of polymer molecules	40	40	40	40	40	40	40
no. of H_2O molecules	4902	4590	4249	3873	3456	2476	1232
no. of CH_3OH molecules	0	312	653	1029	1446	2426	3670
no. of H_3O^+ molecules	400	400	400	400	400	400	400
cell size (Å)	74.9	75.5	76.1	76.9	77.8	79.6	81.9
density (g/cm^3)	1.72	1.69	1.67	1.64	1.61	1.54	1.47

[a] See ref 32.

were truncated at 10 Å, and long-range energy corrections were taken into account. It is assumed that one polymer consists of 10 monomers, which are composed of 16 CF_2 groups in the main chain ($x = 7$, $y = 1$) and the sulfonic-type pendant side chain ($m = 1$, $n = 2$) shown in Figure 1. The polymer chain is composed of ether oxygen and united atoms, such as CF_3, CF_2, and CF. The force field parameters for the united atoms were taken from models of Cui et al.[39,40] and Li et al.,[41] and those for several dihedral angles, such as CF_2-CF_2-S-O, $O-CF_2-CF_2-S$, and $O-CF_2-CF_2-O$, were the same as those in our previous study.[32] Sulfonic acid groups were treated as all-atom models by using OPLS-AA force fields.[42] The flexible TIP3P model[43,44] was applied for water. For methanol, the three interaction sites model proposed by Honma et al.[45] was utilized for the intermolecular potentials, except for spring constants of $O-H$, $O-CH_3$ bondings, and CH_3-O-H bending. They were taken from OPLS-AA potentials.[42] H_3O^+ is used as a counterion of sulfonic acids.

All MD simulations were performed at 358.15 K and 0.1 MPa with a periodic boundary condition using *MPDyn*, coded by Shinoda.[46] The Andersen method[47] was utilized for pressure control, and the Nosé−Hoover chain[48] was used as a thermostat of the system. Equations of motion were integrated by using the rRESPA algorithm[49] with multiple time steps. The Ewald reciprocal forces, the real space nonbonded forces, and the intermolecular interactions were updated at every 2.0, 1.0, and 0.2 fs, respectively. Each MD simulation was performed over a period of at least 1.3 ns, and every final 300 ps, trajectories (6,000 configurations) were used for the analyses.

3. Results and Discussion

A. Membrane Morphology. *(1) Shape of Solvent Clusters.* Figure 2 shows final snapshots of MD simulations. We can recognize from these pictures that solvents form continuous clusters and polymer aggregation in all cases. To estimate the size of the solvent cluster, the structure factor ($S(q)$) of solvent oxygen atoms was calculated as the Fourier transform of the partial radial distribution function (RDF; $g(r)$) for oxygen atoms in both water and methanol as follows:

$$S(q) = 1 + 4\pi\frac{N}{V}\int [g(r) - 1]\frac{\sin(qr)}{q} r\, dr \qquad (1)$$

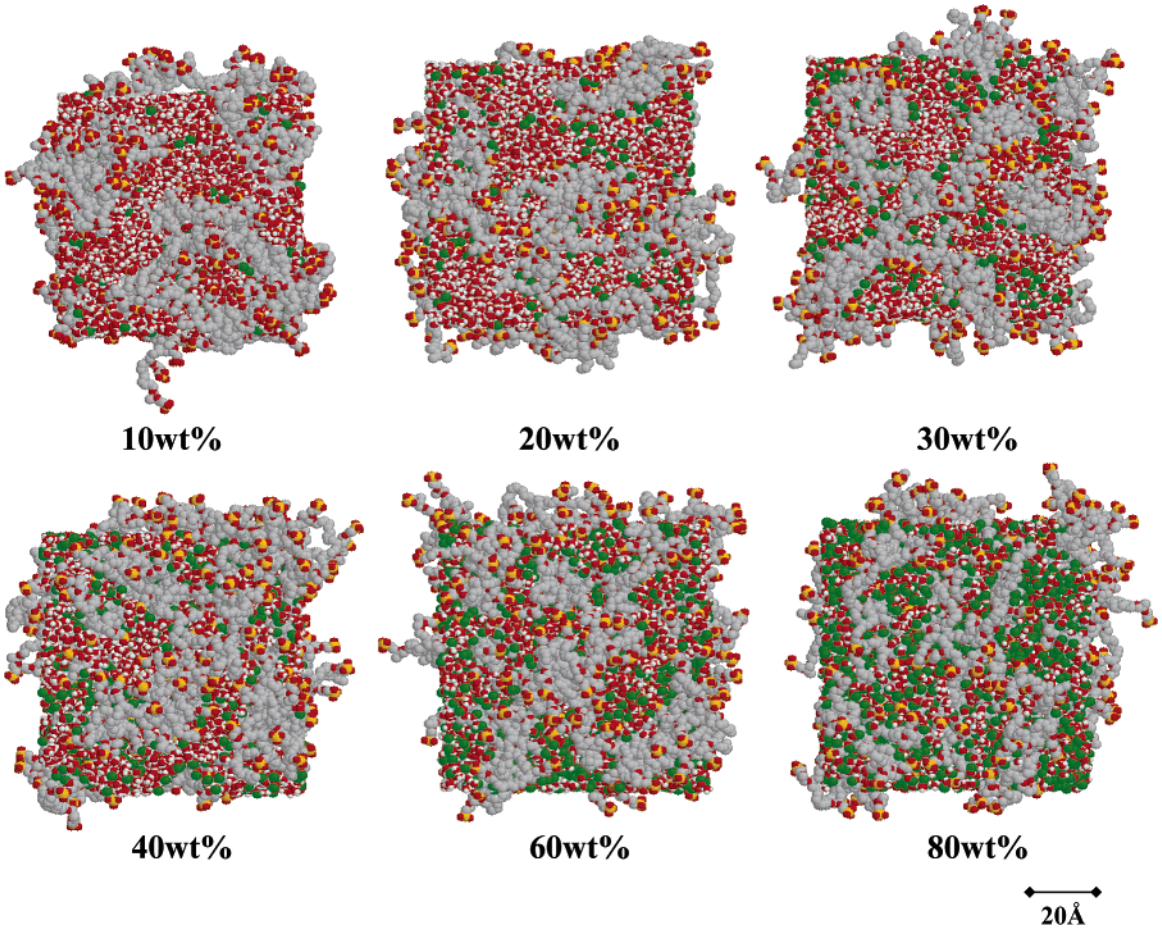

Figure 2. Final snapshots of MD simulations for the membrane immersed in 10−80 wt % methanol concentrations of solution: (red) oxygen atoms, (gray) CF_x groups ($x = 1, 2, 3$), (yellow) sulfur, (white) hydrogen, and (green) methyl group of methanol.

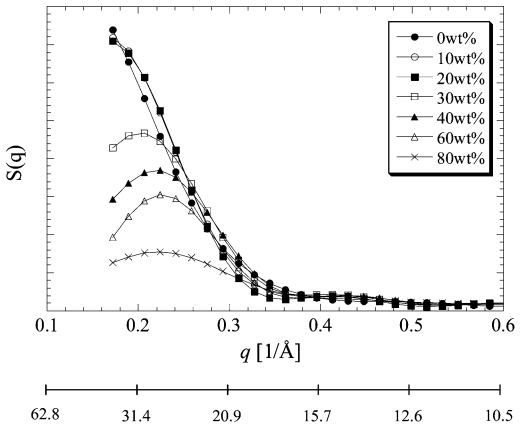

Figure 3. The structure factors estimated as Fourier transform of radial distribution functions for solvent oxygen.

The profiles of $S(q)$ are shown in Figure 3. In the water-uptake membranes, a clear peak around $q = 0.2$ Å^{-1} ($r = 2\pi/q \approx 30$ Å), which represents the solvent cluster, is observed. The peak corresponds to the typical diffraction peak observed experimentally by SANS and SAXS for perfluorinated ionomers.[2−12] The peak height gradually decreases and the distribution becomes broader with increasing methanol concentration. Accordingly, it is known that a higher concentration of methanol solution makes the boundary between the aggregations of polymer matrixes and solvents ambiguous. In addition, this result implies that the solvent cluster becomes nonspherical and the narrow solvent aggregation region increases with increasing methanol concentration in solution, even though the membrane expands more because of higher methanol concentration, as shown in Table 1. On the basis of experimental measurements by electron spin resonance (ESR) and electron nuclear double resonance (ENDOR),[18−20] Schlick and co-workers concluded that the size of the solvent cluster in the membrane swelling in methanol and methanol solution was less than 20 Å. The observed cluster size was smaller than that in water-uptake membranes. The computationally calculated cluster size is somewhat larger than that estimated from the experiments. On the contrary, in the case of water-uptake membranes, the computationally estimated cluster size would be less than that in experimental observations, such as SAXS and SANS.[32] It is therefore difficult to make quantitative comparisons with experiments. However, our simulation result would be approximately in agreement with the experimental observations because the inclination that the cluster should shrink with the addition of methanol is reasonably reproduced.

In the next section, we will analyze the methanol effect on the solvent coordination site to elucidate the reasons for the above phenomenon; higher methanol concentration causes formation of less-spherical solvent clusters.

(2) Solvent Coordination. First, we estimated the coordination number of solvents around each unit of the pendant side chain (Figure 4). The coordination number is defined as the number of molecules that is found within the distance of 4.5 Å from the chain sites. This cutoff distance approximately corresponds to the first minimum of partial RDF between sulfur and solvent oxygen. As a result, it is analogous for all methanol concentrations that solvent molecules highly concentrate in the vicinity of the headgroup, SO_3^-, and the coordination probability of solvent molecules decreases with approach toward the main chain (from left to right in Figure 4) despite the inherent hydrophobic nature of the methyl group of methanol. This is because both intermolecular interaction energies of water and

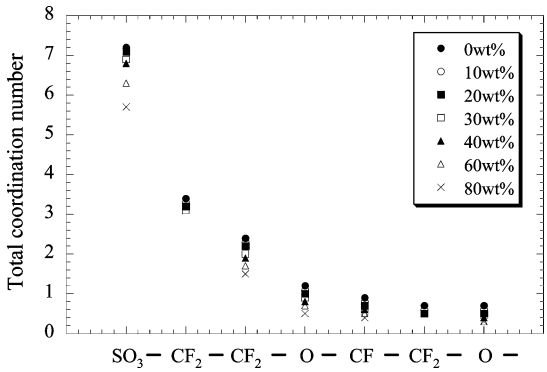

Figure 4. Solvent coordination numbers along the side chain evaluated from the RDFs within the distance of 4.5 Å.

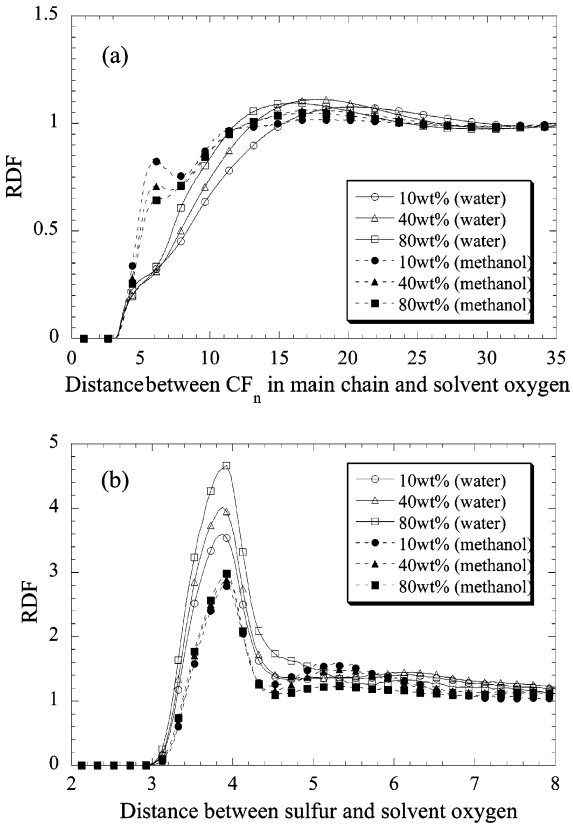

Figure 5. Partial radial distribution functions (a) between polymer main chains and solvents and (b) between sulfur and solvents at 10, 40, and 80 wt % methanol concentrations.

methanol with the sulfonic acid group are almost the same (the interaction energies are −10.52 and −10.38 kcal/mol for the most stable configuration of $CF_3OCF_2CF_2SO_3^- + H_2O$ and $CF_3OCF_2CF_2SO_3^- + CH_3OH$ at the MP2/aug-cc-pVDZ//B3LYP/6-31+G* level[50−56] of molecular orbital calculations[24,29]). Thus, the associations of methanol with the sulfonic acids are much more energetically favorable than those with the other sites in the chain, such as CF_3 and ether oxygen.

However, it is also interesting to point out, from the partial RDF profiles between solvent oxygen and fluorocarbons of the main chain in Figure 5a, that methanol can approach closer to the polymer chain in comparison with water. On the other hand, water associates with the sulfonic acid group more preferably in comparison with methanol (Figure 5b). The methanol mole ratio within the distance of 4.5 Å from the acidic site is about 75% of the overall methanol ratio in all cases. According to the above results, it is revealed that methanol distribution in the membrane swelling in the water/methanol mixture is not

TABLE 2: Ratios of Bonded (BS), Loosely Bonded (LS), and Free (FS) Solvent Molecules in %

	water			methanol			total		
	BS	**LS**	**FS**	**BS**	**LS**	**FS**	**BS**	**LS**	**FS**
0 wt %	45	47	8				45	47	8
10 wt %	46	47	7	39	59	3	46	48	6
20 wt %	46	46	8	39	58	4	45	47	8
30 wt %	47	49	4	37	61	2	45	51	4
40 wt %	47	48	5	36	61	3	44	52	4
60 wt %	48	48	5	35	62	4	41	55	4
80 wt %	47	46	7	32	61	7	35	57	7

TABLE 3: Residence Times (ps) of Bonded (BS) and Loosely Bonded (LS) Solvent Molecules

	0 wt %	10 wt %	20 wt %	30 wt %	40 wt %	60 wt %	80 wt %
				Water			
BS	4.0	3.8	4.0	4.1	4.3	4.5	5.8
LS	2.6	2.5	2.4	2.9	3.0	3.2	3.7
				Methanol			
BS		3.6	3.5	3.7	3.8	4.1	4.7
LS		4.4	4.2	5.0	5.3	5.6	6.2

the same as that of in water because of the different nature in affinity between water and methanol.

We can also ensure such a view by the following analysis. We classify solvent molecules into three categories: free solvent (**FS**), bonded solvent (**BS**), and loosely bonded solvent (**LS**). We define **FS** as the solvent molecules associating only with solvent molecules within the radius of 6.0 Å. Solvent molecules associating with the sulfonic acids within 4.5 Å are categorized as **BS**, and the other solvents are categorized as **LS**. The analyzed result is summarized in Table 2. A clear difference is observed between water and methanol; the number of **LS** is larger than that of **BS** for methanol, whereas the amount of **LS** is almost the same as that of **BS** for water. Because **LS** should represent the solvent molecules in the narrow channel of solvents or those located near the polymer matrix, this observation shows that methanol prefers to be located near a hydrophobic region. As a result, the increase of methanol concentration enhances the solvent penetration near a polymer matrix composed of fluorocarbons because the overall ratio of **BS** decreases while **LS** increases with increasing methanol content. This result also demonstrates that a less-spherical solvent cluster forms in the membrane swelling in higher methanol concentration of solution, and it supports the results displayed in Figure 3.

Table 3 summarizes residence times of solvents in two locations, **BS** and **LS**. These were evaluated using the following correlation function

$$C(s,t) = \frac{\langle h_i(s,t)\, h_i(s,0)\rangle}{\langle h_i(s,0)\, h_i(s,0)\rangle}, \qquad (2)$$

where $h_i(s,t)$ was defined as unity if the water molecule i was found in the location s during $t = 0 \sim t$; otherwise $h_i = 0$. The residence time was evaluated by using the numerical integration of the correlation function, with a correction by fitting the tail region of the correlation function to a single, exponential one. (Here, the residence time of **FS** was not estimated because the number of **FS** is too scarce to be analyzed.) Different characteristics were observed between water and methanol; a water molecule stays longer at a **BS** site than at a **LS** site, and methanol resides longer at a **LS** site than at a **BS** site.

In conclusion, it is suggested that methanol contributes to polymer−solvent separation in the membrane of perfluorosulfonic acid ionomers, as in the case of water, because of the strong interaction with the sulfonic acid group by O−H···O hydrogen bonding. However, the cluster shape gradually becomes less spherical as a function of methanol concentration. This is because methanol penetrates into a polymer matrix more than water because of the hydrophobic nature of the methyl group.

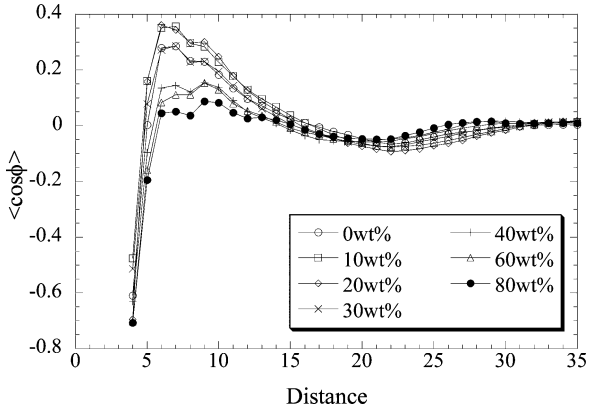

Figure 6. Orientational correlation of the pendant side chains, $\langle \cos \varphi_{ij}(t)\rangle = \langle \mathbf{s}_i(t)\cdot\mathbf{s}_j(t)\rangle$, as a function of the distance between sulfur atoms. The side chain direction **s** was defined as a vector from the end side of the side chain (CF group) to the sulfur atom.

(3) Polymer Structure. In this subsection, we investigate polymer structure change as a function of methanol concentration. According to the RDF profiles of sulfurs, the second sulfur was found in proximity of the first sulfur within 6.8, 6.9, 7.1, 7.3, 7.6, and 7.5 Å for the membranes in 10, 20, 30, 40, 60, and 80 wt % methanol solutions, respectively. This trend indicates that the average distance between sulfonic acid groups is slightly but gradually increased with increasing methanol concentration. In the case of water-uptake membranes, the distance spreads depending on the amount of water absorbed because water clusters aggregate with increasing water content.[32] Contrarily, in the case of methanol solution, the reason for the longer distance between neighboring sulfurs is not growth of the solvent cluster because its shape becomes broader with increasing methanol ratio, as discussed above. A possible reason is that the polymer chain is unraveled in a higher methanol concentration of solution. A larger radius of gyration of a polymer chain was observed for the higher methanol concentration in our calculations; the radius increases to 544.4, 541.2, 545.1, 554.9, 559.0, 577.5, and 580.9 Å^2 for 0, 10, 20, 30, 40, 60, and 80 wt % methanol concentrations, respectively. This trend is analogous with the MD simulations of an oligomer of Nafion in water, water/methanol, and methanol, which have been reported by Vishnyakov and Neimark.[22,23] They found that the oligomer formed spherical configurations in water, whereas it spread in methanol and water/methanol mixtures. SAXS observations of dilute solutions of the ionomer in a series of solvents have also shown that the polymer aggregation is larger in water than in methanol.[57]

Next, we analyzed the correlation of the orientations of pendant side chains, i and j, as a function of their distance;

$$\langle \cos \varphi_{ij}(t)\rangle = \langle \mathbf{s}_i(t)\cdot\mathbf{s}_j(t)\rangle \qquad (3)$$

where **s** is a vector that directs from the end tail of the side chain (CF group connects with main chain) to the sulfur of the headgroup. The result is graphically displayed in Figure 6. All of these profiles showed a broad peak around 5−10 Å, indicating that the side chains within this range tend to direct in the same direction as each other. It is observed that the peak height monotonically decreases with the increase of methanol concentration, representing a less-ordered polymer structure immersed

TABLE 4: Number of Hydrogen Bonds between Sulfonic Acid Oxygen (O_s) and an O−H Group of Solvent Molecules[a]

methanol concn	water	methanol	H_3O^+	total
10 wt %	3.2 (0.2)	0.1	0.2	3.5
20 wt %	3.0 (0.2)	0.3	0.2	3.5
30 wt %	2.8 (0.2)	0.5	0.2	3.4
40 wt %	2.5 (0.2)	0.7	0.2	3.4
60 wt %	1.9 (0.1)	1.2	0.2	3.2
80 wt %	1.1 (0.1)	1.7	0.2	2.9

[a] The number of water molecules forming two O_s···H−O bonds is in parentheses.

in a higher methanol concentration of solution. Another finding is that the minimum position appearing around 20−25 Å is shorter in a higher methanol concentration. It represents a narrower solvent cluster and/or a more spread structure of the polymer chain because of more methanol absorption. These results support the above discussions that a higher methanol concentration causes less clear polymer/solvent separation and narrower clusters that are partially formed in the membrane. We also notice the negative value of cos φ at 4 Å, which is observed in all the conditions, interpreting the existence of a very narrow space sandwiched by the pendant side chains orientating opposite directions from each other. Such a fact has also been observed for 5−40 wt % water-swollen membranes in our previous MD study.[32]

B. Hydrogen Bonding. Next, hydrogen bonding between sulfonic oxygen (O_s) and an O−H group of solvents (O_s···H−O) was analyzed to investigate local solvation structure around the acidic site. We noticed that hydrogen bonds are formed when the distance between hydrogen and O_s is less than 2.0 Å and the angle of O_s···H−O is over 120°. Table 4 summarizes the number of hydrogen bonds per sulfonic acid group. The number of water molecules forming the O_s···H−O monotonically decreases, and that of methanol increases as a function of methanol concentration. In Table 5, water (x_W) and methanol (x_M) mole ratios in the solvent molecules forming the O_s···H−O hydrogen bonds are shown (H_3O^+ is considered). Mole ratios of water and methanol in overall solution (ρ_W and ρ_M,respectively) and those within a 4.5 Å distance of sulfur (c_W and c_M, respectively) are also listed. The normalized concentration of water forming O_s···H−O, that is, x_W/ρ_W, increases with increasing methanol concentration, as in the case of c_W/ρ_W, indicating that water more highly concentrates to the sulfonic acid group and forms hydrogen bonds with the acidic site at higher methanol concentrations of solution. In the case of methanol, both x_M/ρ_M and c_M/ρ_M are less than unity. However, it is interesting to note that only x_M/ρ_M increases with an increase of methanol concentration of solution.

So, to understand this phenomenon, we analyzed an averaged distribution of the angle between O_s and the O−H group (O_s···H−O), whose hydrogen exists within 2.0, 2.5, and 3.0 Å distances of O_s ($R_{Os\cdots H}$). These results are graphically shown in Figure 7. For methanol, a higher peak was observed at higher methanol concentration in the range of about 160−170° for all cases, showing that methanol forms more linear O_s···H−O bonds at higher methanol concentration. In addition, for the cutoff of $R_{Os\cdots H}$ = 3.0 Å, a higher peak appeared at around 60°, which would correspond to methanol in the second solvation shell at a lower methanol concentration of solution.

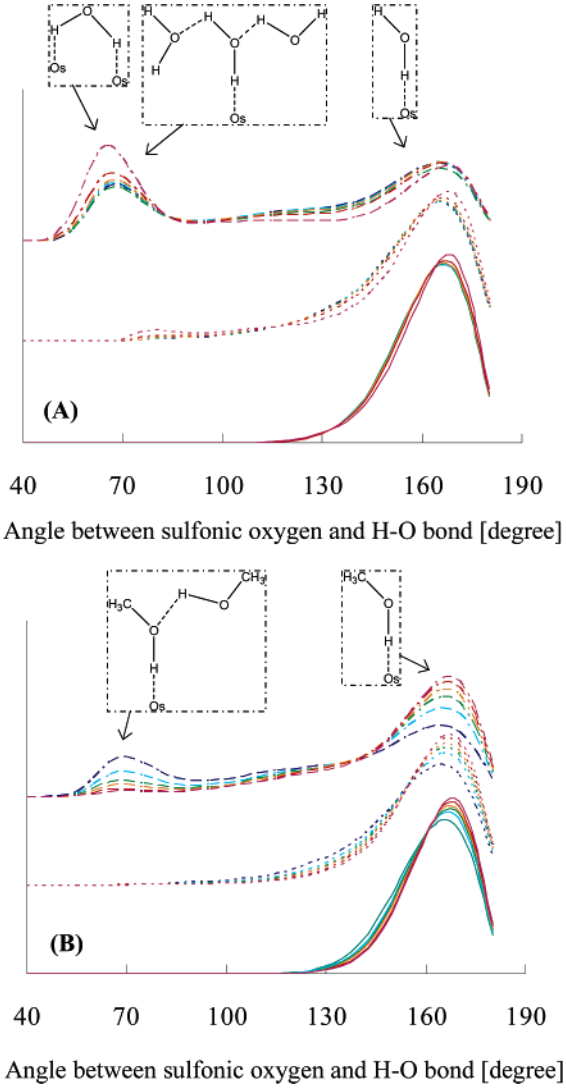

Figure 7. Normalized distribution of the angle between sulfonic oxygen (O_s) and the O−H group of solvents (Os···H−O) within the distances 2.0 (lower), 2.5 (middle), and 3.0 (upper) Å from O_s: (A) water and (B) methanol in (blue) 10 wt %, (light blue) 20 wt %, (green) 30 wt %, (yellow) 40 wt %, (red) 60 wt %, and (purple) 80 wt % methanol concentrations. Inserts are schematic illustrations of hydrogen bonding.

TABLE 5: Mole Ratios of Water and Methanol in Overall Solution (ρ_W and ρ_M, Respectively), Those in the Solvent Molecules Forming the O_s···H−O Hydrogen Bonds (x_W and x_M, Respectively), and Those within a 4.5 Å Distance of Sulfur (c_W and c_M, Respectively)[a]

methanol concn of solution	molecules in overall solvent (mol ratio)		molecules within 4.5 Å of sulfonic acid (mol ratio)		molecules forming hydrogen bonds with O_s (mol ratio)					
	water (ρ_w)	methanol (ρ_M)	water (c_w)	methanol (c_M)	water (x_w)	methanol (x_M)	c_w/ρ_w	x_w/ρ_w	c_M/ρ_M	x_M/ρ_M
10 wt %	0.87	0.06	0.86	0.04	0.90	0.03	0.99	1.04	0.74	0.55
20 wt %	0.80	0.12	0.80	0.09	0.84	0.09	1.00	1.05	0.75	0.70
30 wt %	0.73	0.19	0.75	0.14	0.79	0.15	1.03	1.08	0.74	0.76
40 wt %	0.65	0.27	0.69	0.20	0.72	0.22	1.06	1.10	0.74	0.79
60 wt %	0.47	0.46	0.53	0.34	0.55	0.38	1.14	1.18	0.75	0.83
80 wt %	0.23	0.69	0.30	0.53	0.35	0.59	1.27	1.50	0.76	0.85

[a] H_3O^+ is considered.

TABLE 6: Diffusion Coefficient and Rotational Relaxation Time for the Three Types of Solvents, Categorized by Bonded (BS), Loosely Bonded (LS), and Free (FS) Solvent Molecules

	diffusion coeff ($\times 10^{-6}$ cm^2/s)			rotational relaxation time (ps)			residence time (ps)	
water	**BS**	**LS**	**FS**	**BS**	**LS**	**FS**	**BS**	**LS**
0 wt %	0.37	0.47	0.62	2.1	1.2	0.7	4.0	2.6
10 wt %	0.36	0.44	0.60	1.9	1.3	0.7	3.8	2.5
20 wt %	0.33	0.41	0.57	2.0	1.4	0.8	4.0	2.4
30 wt %	0.32	0.39	0.48	2.1	1.5	1.0	4.1	2.9
40 wt %	0.29	0.35	0.44	2.3	1.7	1.1	4.3	3.0
60 wt %	0.24	0.31	0.35	2.8	2.2	1.5	4.5	3.2
80 wt %	0.19	0.26	0.38	4.2	3.3	2.1	5.8	3.7
	diffusion coeff ($\times 10^{-6}$ cm^2/s)			rotational relaxation time (ps)			residence time (ps)	
methanol	**BS**	**LS**	**FS**	**BS**	**LS**	**FS**	**BS**	**LS**
10 wt %	0.22	0.26	0.38	2.8	1.9	0.7	3.6	4.4
20 wt %	0.21	0.26	0.41	2.9	1.9	0.8	3.5	4.2
30 wt %	0.22	0.26	0.37	2.8	1.9	1.0	3.7	5.0
40 wt %	0.21	0.25	0.34	2.7	1.8	1.0	3.8	5.3
60 wt %	0.20	0.25	0.31	2.8	2.0	1.2	4.1	5.6
80 wt %	0.19	0.24	0.33	3.3	2.3	1.4	4.7	6.2

It is thus expected that a higher methanol concentration of solution causes methanol to form more $O_s\cdots H-O$ hydrogen bonds.

In the case of water, there is no clear methanol concentration dependence on the profile for $R_{H\cdots Os} < 2.0$ Å. In this range, only the O−H groups directly interacting with O_s are included. In the case of $R_{H\cdots Os} < 2.5$ Å, a small peak appears at about 60° only for 80 wt % methanol concentration. This peak is enhanced at all concentrations when the cutoff of $R_{H\cdots Os}$ is set to 3.0 Å, and the peak height at 60° is obviously higher at a higher methanol concentration, especially for 80 wt %; the peak is higher by 160−170°. The peak at 60° was assigned to another hydrogen atom of a pair that form the $Os\cdots H-O$ hydrogen bond or a hydrogen atom of another water molecule in the second solvation shell. Within a distance of 2.5 Å, the former would be responsible for the peak at 60°; therefore, we can guess that the water molecule prefers to direct its two O−H groups toward the acidic headgroup in such a way that the water avoids interacting with methanol-rich solvent. These orientation changes of water and methanol provide explanations for the result that x_M/ρ_M increases as a function of methanol concentration.

C. Solvent Dynamics. Effective diffusion coefficients and rotational relaxation times of the solvents are displayed in Figure 8. The diffusion coefficient was evaluated from the mean square displacement as follows:

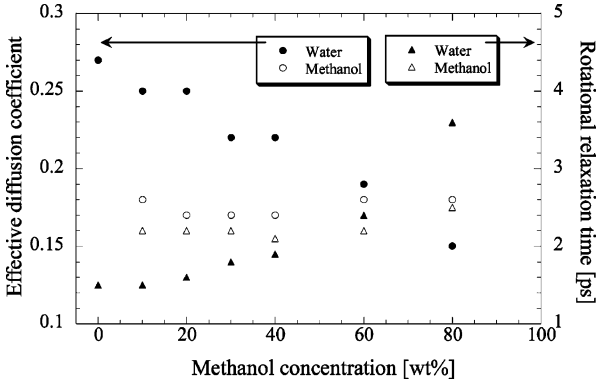

Figure 8. Diffusion coefficients ($\times 10^{-6}$cm^2/s) and rotational relaxation times (ps) of water and methanol.

$$D = \frac{\langle |r(t) - r(0)|^2 \rangle}{6t} \quad (4)$$

The rotational relaxation time was estimated using the rotational correlation function defined as

$$C(t) = \left\langle \frac{1}{2}[3\cos^2\theta(t) - 1] \right\rangle = \frac{1}{2}\langle 3[d_i(t)\cdot d_i(0)]^2 - 1 \rangle \quad (5)$$

where $d_i(t)$ is the vector of the dipole axis and that of the angle bisector of CH_3-O-H for water and methanol, respectively. The relaxation time was evaluated in the same manner as residence relaxation time. As a result, the water diffusion coefficient monotonically decreases and the relaxation time increases with increasing methanol content. On the contrary, methanol diffusion and rotation do not change much. It is thus inferable that steady mobility of methanol occurs in overall solvent dynamics.

On the other hand, it is interesting that water mobility is constrained more in comparison with methanol at 80 wt % methanol concentration. To investigate the cause of this constrained mobility, diffusion coefficients and rotational relaxation times for the three types of solvent molecules categorized into **BS**, **LS**, and **FS** were analyzed. The calculated results are summarized in Table 6. Here, the effective diffusion coefficients for the three categories were estimated by using short-time trajectory data from 3 to 10 ps because the time scale that a solvent molecule is localized in the same region is very short. Methanol diffusion and rotation for the three locations change little, and those of water systematically depend on methanol concentration and approach the values of methanol. These phenomena are consistent with the overall dynamic properties. It is evident that solvent dynamics depends on the location; the mobility order is **FS** > **LS** > **BS**. As previously mentioned, the number of **BS** of water is almost the same as that of **LS** of water, and the number of **LS** of methanol is more than that of **BS** of methanol. Therefore, a possible reason water is less mobile than methanol at high methanol concentrations is the difference of preferable locations for water and methanol.

4. Conclusions

The swollen membranes of a perfluorosulfonic ionomer in 10−80 wt % methanol concentrations of solutions were investigated by means of molecular dynamics simulation. In this study, we assumed the same number of solvent molecules as with 20 wt % water-uptake membranes, which have been studied in our previous work,[32] to elucidate the methanol concentration dependence of membrane morphology.

According to the statistical structure factors evaluated as a Fourier transform of a partial RDF profile of solvent oxygen, we found that the peak representing the cluster size shifts toward a larger q value and gets broader with increasing methanol concentration. This implies that a less-spherical solvent cluster is formed in the membrane immersed in a higher methanol concentration of solution. We presume that this phenomenon is due to the ampholytic nature of methanol. Indeed, RDF profiles between solvent oxygen and fluorocarbons constructing a main chain clearly show that methanol can more easily approach a hydrophobic polymer matrix in comparison with water. Also, water is preferentially located in the vicinity of the acidic headgroup, SO_3^-, compared with methanol, even though both have similar attractive interaction energies to the acidic group. The methanol effect on polymer structure was also analyzed, and we observed a larger radius of gyration of a polymer chain for the higher methanol concentration. Additionally, according to correlation of two pendant side chain directions as a function of their distance, it was confirmed that methanol makes polymer aggregation less spherical. These results are qualitatively in agreement with experiments of SAXS,[21,57] ESR, and ENDOR.[18−20]

The shape of hydrogen bonds between a solvent O−H group and sulfonic acid oxygen (O_s···H−O) also depends on methanol concentration: methanol forms more linear O_s···H−O bonds at higher methanol concentration, and a water molecule prefers to direct its two O−H groups toward the acidic headgroup in such a way that the water avoids interacting with methanol-rich solvent.

The effective diffusion coefficient and the rotational relaxation time of solvents were also analyzed. It is interesting to note that solvent dynamics clearly depends on their position. A solvent coordinating to the acidic site is most immobile, and those in the center of a solvent cluster are relatively mobile. The solvent near a polymer chain or in a narrow channel shows moderate mobility. Such a location dependence of the solvent dynamics is attributed to the lower mobility of water in comparison with that of methanol at the membrane immersed in higher methanol concentration because water is bound to the acidic site more strongly than methanol.

References and Notes

(1) Tant, M. R.; Mauritz, K. A.; Wilkes, G. L. *IONOMERS*; Blackie Academic & Professional: London, New York, 1997.
(2) Fujimura, M.; Hashimoto, T.; Kawai, H. *Macromolecules* **1981**, *14*, 1309.
(3) Fujimura, M.; Hashimoto, T.; Kawai, H. *Macromolecules* **1982**, *15*, 136.
(4) Gierke, T. D.; Munn, G. E.; Wilson, F. C. *J. Polym. Sci., Polym. Phys. Ed.* **1982**, *19*, 1687.
(5) Roche, E. J.; Pineri, M.; Duplessix, R.; Levelut, A. M. *J. Polym. Sci., Polym. Phys. Ed.* **1981**, *19*, 1.
(6) Heaney, M. D.; Pellegrino, J. *J. Membr. Sci.* **1989**, *47*, 143.
(7) Elliott, J. A.; Hanna, S.; Elliot, A. M. S.; Cooley, D. E. *Macromolecules* **2000**, *33*, 4161.
(8) Gebel, G. *Polymer* **2000**, *41*, 5829.
(9) James, P. J.; Elliott, J. A.; McMaster, T. J.; Newton, J. M.; Elliott, A. M. S.; Hanna, S.; Miles, M. J. *J. Mater. Sci.* **2000**, *35*, 5111.
(10) Lehmani, A.; Durand-Vidal, S.; Turo, P. *J. Appl. Polym. Sci.* **1998**, *68*, 503.
(11) Rollet, A.-L.; Diat, O.; Gebel, G. *J. Phys. Chem. B* **2002**, *106*, 3033.
(12) Porat, Z.; Fryer, J. R.; Huxham, M.; Rubinstein, I. *J. Phys. Chem.* **1995**, *99*, 4667.
(13) Chomakova-Haefke, M.; Nyffenegger, R.; Schmidt, E. *Appl. Phys. A* **1994**, *59*, 151.
(14) Kuver, A.; Vielstich, W. *J. Power Sources* **1998**, *74*, 211.
(15) Ravikmar, M. K.; Shukla, A. K. *J. Electrochem. Soc.* **1996**, *143*, 2601.
(16) Heinzel, A.; Barragán, V. M. *J. Power Sources* **1999**, *84*, 70.
(17) Cruickshank, J.; Scott, K. *J. Power Sources* **1998**, *70*, 40.
(18) Schlick, S.; Alonso-Amigo, M. G. *Macromolecules* **1989**, *22*, 2634.
(19) Schlick, S.; Alonso-Amigo, M. G.; Bednarek, J. *Colloids Surf., A* **1993**, *72*, 1.
(20) Li, H.; Schlick, S. *Polymer* **1995**, *36*, 1141.
(21) Haubold, H.-G.; Vad, Th.; Jungbluth, H.; Hiller, P. *Electrochim. Acta* **2001**, *46*, 1559.
(22) Vishnyakov, A.; Neimark, A. V. *J. Phys. Chem. B* **2001**, *105*, 7830.
(23) Vishnyakov, A.; Neimark, A. V. *J. Phys. Chem. B* **2000**, *104*, 4471.
(24) Urata, S.; Irisawa, J.; Takada, A.; Tsuzuki, S.; Shinoda, W.; Mikami, M. *J. Fluorine Chem.*, accepted for publication.
(25) Khalatur, P. G.; Talitskikh, S. K.; Khokhlov, A. R. *Macromol. Theory Simul.* **2002**, *11*, 566.
(26) Mologin, D. A.; Khalatur, P. G.; Khokhlov, A. R. *Macromol. Theory Simul.* **2002**, *11*, 587.
(27) Krueger, J. J.; Simon, P. P.; Ploehn, H. J. *Macromolecules* **2002**, *35*, 5630.
(28) Vishnyakov, A.; Neimark, A. V. *J. Phys. Chem. B* **2001**, *105*, 9586.
(29) Urata, S.; Irisawa, J.; Takada, A.; Tsuzuki, S.; Shinoda, W.; Mikami, M. *Phys. Chem. Chem. Phys*. **2004**, *6*, 3325.
(30) Groot, R. D.; Warren, P. B. *J. Chem. Phys.* **1997**, *107*, 15.
(31) Jang, S. S.; Molinero, V.; Çağin, T.; Goddard, W. A., III. *J. Phys. Chem. B* **2004**, *108*, 3149.
(32) Urata, S.; Irisawa, J.; Takada, A.; Tsuzuki, S.; Shinoda, W.; Mikami, M. *J. Phys. Chem. B* **2005**, *109*, 4269.
(33) Paddison, S. J. *Annu. Rev. Mater. Res.* **2003**, *33*, 289.
(34) Paddison, S. J.; Pratt, L. R.; Zawodzinski, T. A., Jr. *J. New Mater. Electrochem. Syst.* **1999**, *2*, 183.
(35) Paddison, S. J.; Paul, R.; Zawodzinski, T. A., Jr. *J. Electrochem. Soc.* **2000**, *147*, 617.
(36) Paddison, S. J. *J. New Mater. Electrochem. Syst.* **2001**, *4*, 197.
(37) Paddison, S. J.; Paul, R. *Phys. Chem. Chem. Phys*. **2002**, *4*, 1158.
(38) Ewald, P. P. *Ann. Phys.* **1921**, *64*, 253.
(39) Cui, S. T.; Siepmann, J. I.; Cochran, H. D.; Cummings, P. T. *Fluid Phase Equilib.* **1998**, *146*, 51.
(40) Cui, S. T.; Cochran, H. D.; Cummings, P. T. *J. Phys. Chem. B* **1999**, *103*, 4485.
(41) Li, H.-C.; Mccabe, C.; Cui, S. T.; Cummings, P. T.; Cochran, H. D. *Mol. Phys.* **2001**, *100*, 265.
(42) Jorgensen, W. L.; Maxwell, D. S.; Tirado-Rives, J. *J. Am. Chem. Soc*. **1996**, *118*, 11225.
(43) Jorgensen, W. L.; Chandrasekhar, J.; Madura, J. P. *J. Chem. Phys.* **1983**, *79*, 926.
(44) Neria, E.; Fisher, S.; Karplus, M. *J. Chem. Phys.* **1996**, *105*, 1902.
(45) Honma, T.; Liew, C. C.; Inomata, H.; Arai, K. *J. Phys. Chem. A* **2003**, *107*, 3960.
(46) Shinoda, W.; Mikami, M. *J. Comput. Chem*. **2003**, *24*, 920. http://staff.aist.go.jp/w.shinoda/index.html.
(47) Andersen, H. C. *J. Chem. Phys.* **1980**, *72*, 2384.
(48) Martyna, G. J.; Tuckerman, M. E.; Klein, M. L. *J. Chem. Phys.* **1992**, *97*, 2638.
(49) Martyna, G. J.; Tuckerman, M. E.; Tobias, D. J.; Klein, M. L. *Mol. Phys.* **1996**, *87*, 1117.
(50) Møller, C.; Plesset, M. S. *Phys. Rev.* **1934**, *46*, 618.
(51) Miehlich, B.; Savin, A.; Stoll, H.; Preuss, H. *Chem. Phys. Lett*. **1989**, *157*, 200.
(52) Fricsh, M. J.; Pople, J. A.; Binkley, J. S. *J. Chem. Phys.* **1984**, *80*, 3265.
(53) Becke, A. D. *J. Chem. Phys.* **1993**, *98*, 5648.
(54) Lee, C.; Yang, W.; Parr, R. G. *Phys. Rev. B* **1988**, *37*, 785.
(55) Kendall, R. A.; Dunning, T. H., Jr.; Harrison, R. J. *J. Chem. Phys*. **1992**, *96*, 6796.
(56) Woon, D. E.; Dunning, T. H., Jr. *J. Chem. Phys.* **1993**, *98*, 1358.
(57) Loppinet, B.; Gebel, G.; Williams, C. E. *J. Phys. Chem. B* **1997**, *101*, 1884.